INTERNATIONAL JOURNAL FOR NUMERICAL METHODS IN FLUIDS, VOL. 4, 303–319 (1984)

ON THE FINITE-ELEMENT CALCULATION OF TURBULENT FLOW USING THE k–ε MODEL

R. M. SMITH

Central Electricity Generating Board, Berkeley Nuclear Laboratories, Berkeley, Gloucestershire GL13 9PB, England

SUMMARY

Although the finite-element (FE) method has been successful in analysing complex laminar flows, a number of difficulties can arise when two-equation turbulence models (e.g. the k–ε model) are incorporated. This work describes a particular FE discretization of the k–ε model and reports its performance in recirculating flow. Severe problems encountered in attempts to obtain convergence of the numerical scheme are isolated and analysed, and methods by which the problems can be overcome are suggested.

Insight gained in this work has enabled a practical turbulent flow FE code to be constructed which is robust and efficient. This code is the subject of a further paper.

KEY WORDS Finite Element Turbulent Flow

1. INTRODUCTION

The finite-element (FE) method has met with considerable success in the solution of problems of laminar flow and related heat transfer.[1,2] Extension to turbulent flow in complex geometry calls for the use of a model of turbulence which can account for the transport of turbulence quantities, since the stresses are not in general locally determined. The so-called two-equation models are the simplest which are suitable for calculations in complex flow. They use the concept of an eddy viscosity which is determined by the solution of two coupled transport equations. The most widely used such model is the k–ε model,[3,4] in which the two transported quantities are the turbulence energy, k and its rate of dissipation, ε. Hitherto, most of the computer codes using this model have been similar to those originally produced at Imperial College.[5] They use hybrid upwind-differencing and solve the resulting equations by under-relaxation methods. There is relatively little experience of the solution of the k–ε equations using the finite-element method.[6–8] The few published results in complex geometry reflect the difficulty of finite-element discretization and subsequent solution of the highly non-linear coupled system.

A previous paper[9] has introduced a particularly convenient finite-element discretization of the k–ε model and reported solutions for simple pipe flows. The purpose of the present paper is to report an extension of the above work to encompass more complex recirculating flow. Particular emphasis is placed on the analysis of certain difficulties encountered in the convergence of the numerical method, and on devising means by which these difficulties can be overcome.

In the following, all variables will be rendered dimensionless with respect to characteristic length L and velocity V (the Reynolds number then being given by $Re = LV/\nu$ where ν is the dynamic viscosity) and the summation convention is used throughout.

0271–2091/84/040303–17$01.70 *Received 3 May 1983*

2. BASIC EQUATIONS FOR THE k–ε MODEL

The equations governing the steady axisymmetric flow of an incompressible turbulent fluid are

$$u_m \frac{\partial u_n}{\partial x_m} + \frac{\partial p}{\partial x_n} - \frac{1}{x_2}\frac{\partial}{\partial x_m}\left(x_2 \pi_u \left(\frac{\partial u_m}{\partial x_n} + \frac{\partial u_n}{\partial x_m}\right)\right) + 2\pi_u \frac{u_2}{x_2^2}\delta_{n2} = 0, \quad \text{for } \mathbf{x} \text{ in } \Omega \tag{1}$$

$$\frac{1}{x_2}\frac{\partial}{\partial x_m}(x_2 u_m) = 0, \quad \text{for } \mathbf{x} \text{ in } \Omega \tag{2}$$

where p is the mean pressure, $\mathbf{u}$ is the mean velocity and δ_{nm} is the Kronecker delta. The velocity components u_1, u_2, are in the axial direction x_1 and the radial direction x_2, respectively. The dimensionless diffusivity of momentum is given by

$$\pi_u = (1 + \mu_t)/Re \tag{3}$$

where μ_t is the dimensionless eddy viscosity.

The above equations are to be solved in region Ω subject to boundary conditions of the form:

$$\mathbf{u} = \hat{\mathbf{u}} \quad \text{for } \mathbf{x} \text{ on } \partial\Omega_1 \text{ (walls, inlet)}$$

$$T_1 = u_2 = 0 \quad \text{for } \mathbf{x} \text{ on } \partial\Omega_2 \text{ (symmetry line)}$$

$$T_1 = T_2 = 0 \quad \text{for } \mathbf{x} \text{ on } \partial\Omega_3 \text{ (general outlet)}$$

where the notation $\hat{\mathbf{u}}$ indicates a prescribed function of $\mathbf{u}$, $\partial\Omega_1$, $\partial\Omega_2$, $\partial\Omega_3$ is a partition of the boundary $\partial\Omega$ and, if $\mathbf{n}$ is the outward pointing unit normal to $\partial\Omega$, the surface traction $\mathbf{T}$ is defined by

$$T_l = \left(-p\delta_{lm} + \pi_u\left(\frac{\partial u_l}{\partial x_m} + \frac{\partial u_m}{\partial x_l}\right)\right) n_m \tag{4}$$

The system is closed by specification of the eddy viscosity. In the k–ε turbulence model, the eddy viscosity is given by the relation

$$\mu_t = ReC_\mu k^2/\varepsilon \tag{5}$$

where C_μ is a constant. The quantities k and ε themselves are governed by the transport equations

$$u_m \frac{\partial k}{\partial x_m} - \frac{1}{x_2}\frac{\partial}{\partial x_m}\left(x_2 \pi_k \frac{\partial k}{\partial x_m}\right) = Q_k \tag{6}$$

$$u_m \frac{\partial \varepsilon}{\partial x_m} - \frac{1}{x_2}\frac{\partial}{\partial x_m}\left(x_2 \pi_\varepsilon \frac{\partial \varepsilon}{\partial x_m}\right) = Q_\varepsilon \tag{7}$$

with the following definitions for the dimensionless diffusivities and sources:

$$\left.\begin{aligned} \pi_k &= \left(1 + \frac{\mu_t}{\sigma_k}\right)\Big/ Re \\ \pi_\varepsilon &= \left(1 + \frac{\mu_t}{\sigma_\varepsilon}\right)\Big/ Re \\ Q_k &= \mu_t S/Re - \varepsilon \\ Q_\varepsilon &= C_\mu C_{\varepsilon 1} kS - C_{\varepsilon 2}\varepsilon^2/k \end{aligned}\right\} \tag{8}$$

where

$$S = \left(\frac{\partial u_n}{\partial x_m} + \frac{\partial u_m}{\partial x_n}\right)\frac{\partial u_n}{\partial x_m} + 2\left(\frac{u_2}{x_2}\right)^2 \tag{9}$$

The constants C_μ, $C_{\varepsilon 1}$, $C_{\varepsilon 2}$, σ_k and σ_ε must be chosen to give the best fit to experimental results. In this work the recommended values 0·09, 1·44, 1·92, 1·0 and 1·3, respectively, have been used.[4] Boundary conditions on the turbulence transport equations are generally of the form:

$$k = \hat{k}, \qquad \varepsilon = \hat{\varepsilon} \quad \text{for } \mathbf{x} \text{ on } \partial\Omega_1$$

$$\frac{\partial k}{\partial x_m} n_m = 0, \qquad \frac{\partial \varepsilon}{\partial x_m} n_m = 0 \quad \text{for } \mathbf{x} \text{ on } \partial\Omega_2 \text{ and } \partial\Omega_3$$

However, as pointed out by Hutton and Smith,[9] it is not convenient to calculate the momentum field right up to a solid wall. Furthermore, the k–ε model is not valid near a wall where viscous effects are important.[10] The 'wall' part of the $\partial\Omega_1$ boundary is therefore understood to be displaced a small distance into the flow where the fluid can be assumed to by fully turbulent. Conditions which match the interior flow to an assumed behaviour near the wall can then be imposed on that boundary. Suitable matching conditions for duct flow are developed in Reference 9. Following a similar procedure, the usual logarithmic law-of-the-wall

$$u^+ = \frac{1}{\kappa}\ln y^+ + C, \qquad y^+ \geq 30 \tag{10}$$

is applied, but with the velocity parallel to the wall u and distance from the wall y scaled according to:

$$u = \frac{\tau_w}{u_k} u^+; \qquad y = \frac{1}{Re u_k} y^+ \tag{11}$$

The constants κ and C are given their usual values 0·419 and 5·45 respectively, τ_w is the wall shear stress and u_k is given by $C_u^{1/4} k^{1/2}$. In a wall equilibrium layer, where production of turbulence energy balances dissipation, u_k is equal to $\sqrt{|\tau_w|}$. The wall condition (equation (10)) is then equivalent to that in Reference 9, where u^+, y^+ are defined by $u = u^+\sqrt{|\tau_w|}$, $y = y^+/Re\sqrt{|\tau_w|}$. However, the present form is preferred for more general flow with recirculation because, even though τ_w vanishes at a reattachment point, equation (10) still provides a sensible boundary condition on u. The condition on the normal velocity component v is

$$v^+ = \frac{\mathrm{d}}{\mathrm{d}x}\left(\frac{1}{Re u_k}\right) y^+ u^+ \tag{12}$$

where x is tangential distance along the wall and $v = \tau_w v^+/u_k$. Again, this is equivalent to the condition derived in Reference 9 in an equilibrium layer. The corresponding matching conditions used for the turbulence quantities are:

$$\frac{\partial k}{\partial y} = 0; \qquad \varepsilon = C_\mu^{1/2}\frac{k u_k}{\kappa y} \tag{13}$$

Thus, it is assumed that there is a constant-k region near the wall where the length scale is given by $C_\mu^{1/2}\kappa y$. It should be noted that it is not being claimed that the above matching conditions are definitive, but merely that they are a physically sensible choice. Most of the conclusions of the present paper are independent of the particular wall functions chosen.

3. NUMERICAL TREATMENT

3.1. *Finite-element discretization*

The Galerkin finite-element method is used to discretize the momentum equations in the usual way,[11] with the continuity constraint being handled by a penalty-augmented Lagrangian-multiplier (PALM) method.[9] It should be noted that no upwind weighting of the convective terms is employed. Eight-noded quadrilateral elements of the serendipity type[12] with quadratic velocity and linear pressure variations are used in the interior of the flow, with special elements at the wall. The former are referred to as 'type 2' whereas the special elements[13] are types 3 and 4. These have cubic velocity variation perpendicular to the wall and extra nodal variables consisting of the normal gradients of velocity on the grid edge (see Figure 1).

A similar Galerkin treatment of the k–ε transport equations can be used, but this leads to great, and probably unnecessary, complication.[9] Two finite-element models of the k–ε turbulence equations are discussed in the present paper, referred to as models I and II respectively according to their treatment of the S variable defined by equation (9). In both models, the k and ε variables are interpolated using the same basis functions used for the velocity components, whereas the quantities π_u, π_k, π_ε, Q_k and Q_ε are all interpolated using serendipity basis functions. In S-model I, S is also interpolated using serendipity basis functions. The usual Galerkin method is then applied to equations (6), (7) and (9) and the algebraic relations (3) and (8) (having eliminated μ_t using equation (5)) are required to be satisfied pointwise at the grid nodes. The advantages of such a formulation are discussed by Hutton and Smith.[9] A disadvantage is that, since equation (9) is solved by the Galerkin method using basis functions which are continuous across element interfaces, the S variable must be introduced explicitly into the computer code, thus increasing the size and the bandwidth of the global solution matrix. The alternative treatment of S (referred to as S-model II) avoids this problem at the cost of lower accuracy on the mesh. It adopts reduced interpolation on the S variable, replacing the original quadratic variation over an element by a constant value given by averaging the right-hand side of equation (9). Accuracy could be maintained by linearly interpolating the S variable at the four Gauss points of the element,[14] but reduced interpolation has other advantages which will emerge in Section 4.2.

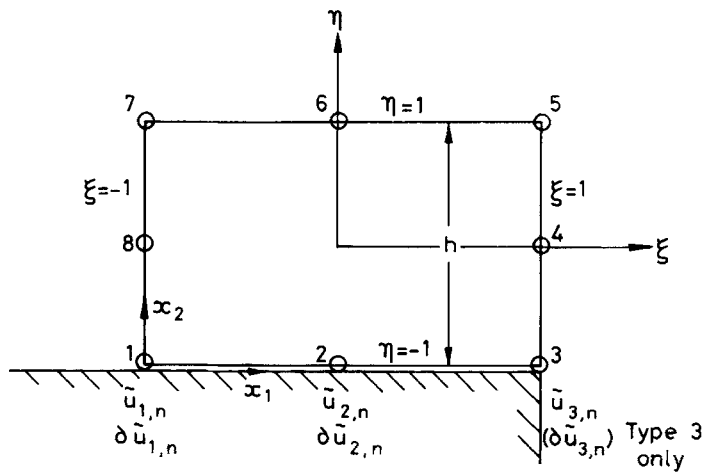

Figure 1. Wall element (type 3 or 4)

The wall matching conditions (10) and (12) are easily incorporated into either scheme using the normal velocity gradients ∂u_i and ∂v_i available at the wall nodes of type 3 and 4 elements. The discrete conditions

$$u_i = \Delta h_i \partial u_i (\ln (C_\mu^{1/4} Re \Delta h_i |k_i|^{1/2}) + \kappa C)$$
$$u_i v_i = \Delta h_i (u_i \partial v_i - v_i \partial u_i)$$

are required to be satisfied at each wall node i, where Δh_i is the displacement of the node from the wall. The second of conditions (13) is also applied pointwise, but $\partial k/\partial y = 0$ is incorporated as a natural boundary condition by leaving k_i free at the wall nodes. This is consistent with an equilibrium wall layer while placing minimum restriction on k where the normal gradient is not strictly zero (e.g. at reattachment where the influence of the external turbulence field extends close to the wall).

3.2. *Solution of the discrete system*

The above procedure (model I or II) results in a non-linear system of algebraic equations which is solved by Newton–Raphson (NR) iteration, using a direct frontal method to handle the linear system at each iteration. It should be noted, however, that k and ε are assumed strictly positive quantities in the transport equations. If they become negative at any point in the iterations, the diffusivities will become negative (equation (5)) and the source terms Q_k and Q_ε (equations (8)) will be completely unphysical. The discrete equations are then highly unstable and divergence of the NR method ensues. This is prevented by substituting the absolute values of the nodal variables of k and ε into the discretized equations. This can destroy the quadratic properties of the iterative scheme since the NR equations are then discontinuous at $k = \varepsilon = 0$, but convergence is quadratic once the iterates remain positive.

The NR method works very well for the momentum equations, an initial guess of zero for all nodal variables usually being sufficient to ensure convergence. The k–ε equations are much more non-linear however, and thus the method is more sensitive to the initial guess. Clearly, if the method is to be of practical use, a guess sufficiently good to ensure convergence must be available. For most flows, reasonable estimates for μ_t and the Prandtl–Kolmorogov length scale l are available. Thus, the following method of starting the numerical solution is proposed:

(i) Guess a μ_t field (a constant, say) and solve the momentum and continuity equations decoupled from the turbulence equations.
(ii) Guess an l distribution (proportional to distance from the wall or a shear layer width, say) and solve the (one equation) k–l transport equation decoupled from the dynamical equations. The single transport equation for k is as equation (6) with $\mu_t \equiv Rek^{1/2}l$ and $\varepsilon \equiv C_\mu k^{3/2}/l$.

The above two steps result in $\mathbf{u}$, p, k and ε fields which are used to initialize the NR iterations on the whole k–ε system.

4. PERFORMANCE OF THE k–ε FINITE ELEMENT CODE

4.1. *Unidirectional flows*

Solutions for both fully-developed and developing pipe flow using S-model I have already been reported in Reference 9. S-model II, as could be expected, requires rather more

elements than S-model I for grid convergence of the k field. In fully developed pipe flow, the errors of S-model II were typically 7 per cent compared with 2 per cent for S-model I on the five element grid in the above Reference. This is not too serious, for the errors introduced by averaging the S term are greatest when k and μ_t are monotonic across the flow (e.g. pipe flow). Also, the mean velocity fields predicted by the two models differed by less than $\frac{1}{2}$ per cent on the above grid, and both were in good agreement with experiment. For both models, convergence of the solution method set out above has been found to be reliable.

4.2. *Recirculating flow*

Recirculating flows present a much more stringent test of both numerical method and turbulence model than those above, particularly in regard to strong turbulence generation in shear layers within the flow and the transport of turbulence away from these areas. The particular example chosen as a test case for the present method is a 1 : 2 diameter-ratio sudden pipe-expansion. A finite-element grid (consisting of 80 elements) and a sketch of the streamline pattern for the flow is shown in Figure 2. Type 3 elements are placed at the centre-line (as well as adjacent to the wall) so that exact symmetry can be imposed, and type 4 elements are used near the re-entrant and concave corners (A and B, respectively) to ensure compatibility of the basis functions. The variables are non-dimensionalized with respect to the downstream pipe diameter and bulk velocity, with Reynolds number taken to be 3×10^4.

The inlet boundary conditions were chosen as follows:

$$u_1=\alpha(1-4x_2)^{1/7}, \qquad u_2=0$$

$$k=k_0, \qquad \varepsilon=\varepsilon_0$$

where the constant α in the Prandtl (1/7) law was chosen to give the correct bulk velocity. The constant inlet values of k and ε were chosen for simplicity, the levels $k_0=0{\cdot}16$ and $\varepsilon_0=0{\cdot}23$ being representative of the turbulence energy and shear stress in the annular inlet of the BNL jet-in-pool experiment.[15]

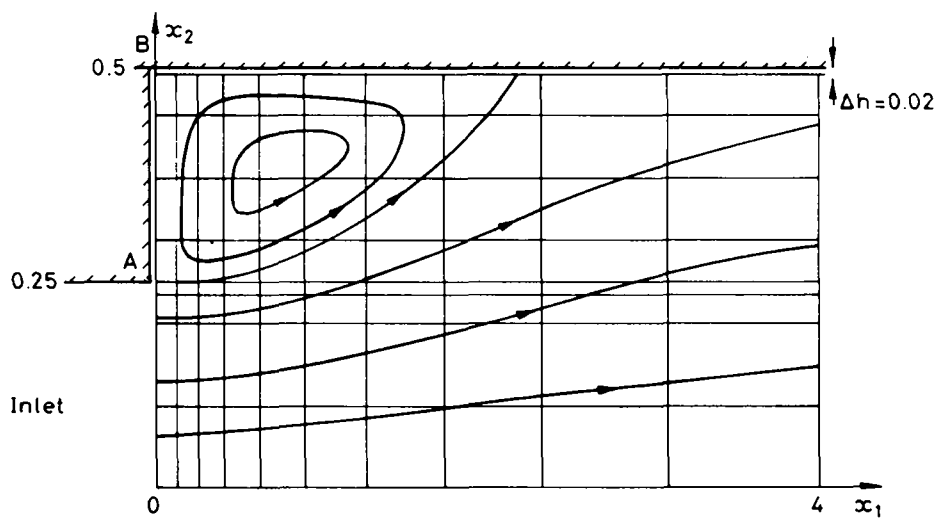

Figure 2. Eighty element grid for the sudden pipe-expansion

A solution for the velocity field with μ_t/Re held constant at 1/70 was easily obtained using NR iteration, the PALM penalty parameter being set to unity for optimum continuity satisfaction. However, attempts to obtain solutions for the turbulence fields with S-model I proved unsuccessful, the procedure described at the end of Section 3 invariably leading to divergence. Furthermore, even if a complete upwind finite-difference solution for the flow (interpolated onto the finite-element mesh) was used as initial guess, the NR method was still found to diverge strongly.

In order to investigate this phenomenon, a series of calculations was carried out (using NR iteration as described earlier) solving the FE k and ε transport equations decoupled from the velocity field, with different specifications of the source term S. The specified velocity field was interpolated from a finite-difference (FD) solution on a uniform mesh of 30×30 nodes, and the S field was calculated from

$$S = (1-\lambda)S'_{FD} + \lambda S_{FE} \tag{14}$$

Here, S'_{FD} was calculated from the FD velocity field using a centred-difference appoximation of equation (9) on the FD mesh, and interpolating to the FE mesh. On the FD nodes around the re-entrant corner however, there are insufficient nodes for a centred-difference approximation, and a quadratic extrapolation from the interior was used instead. Since the velocity gradients near the corner are very high, this will underestimate S in that region. S_{FE} is the result of a Galerkin FE solution of equation (9) using the interpolated FD velocity field in the right-hand side. Thus, as λ is varied from zero to unity in equation (14), S varies from the modified FD approximation to the full FE approximation on the same velocity field. The

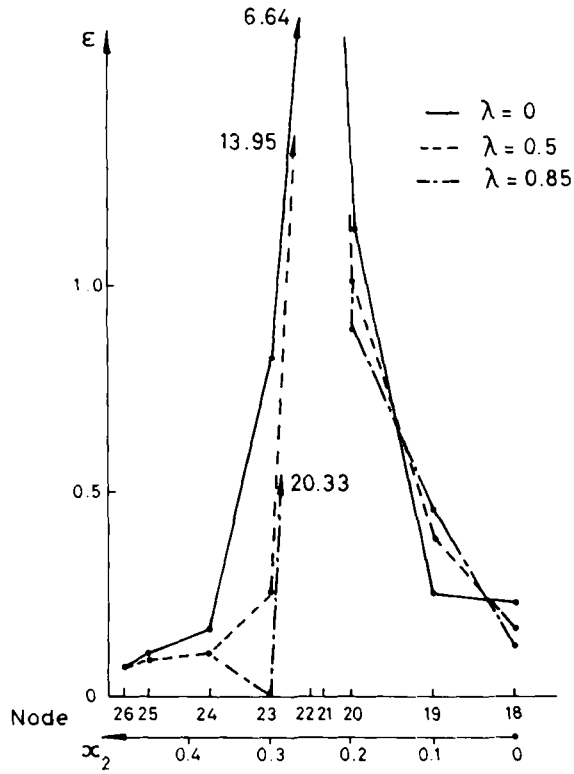

Figure 3. FE solution of k–ε decoupled from the velocity field: variation of ε across the inlet ($x_1 = 0{\cdot}08$)

largest differences between the two occur near the re-entrant corner for the reasons given above. The ratio S_{FE}/S'_{FD} is of order 30 at the corner. The results of these calculations are illustrated by the profiles of ε just downstream of the expansion face shown in Figure 3. As λ is increased the peak value of ε increases drastically in response to the increase of S near the corner. The mesh is too coarse to model such variation, and the overshoot on node 23 eventually takes the value near zero. No solution is possible for $\lambda > 0{\cdot}85$; the iterative scheme oscillates (or diverges if iterates are allowed to go negative).

It is clear from this that the discrete system of equations resulting from S-model 1 has no real solution on the given mesh. The localized peak of S near the re-entrant corner leads to a peak in ε (and k) which, if it cannot be resolved by the mesh, tends to overshoot negative. This destroys the ellipticity of the problem, which then may have no solution.

Overshoot, such as that described above, can be reduced by damping the k and ε fields with artificial diffusion. An alternative is to limit the size of the peak in S to a level where the

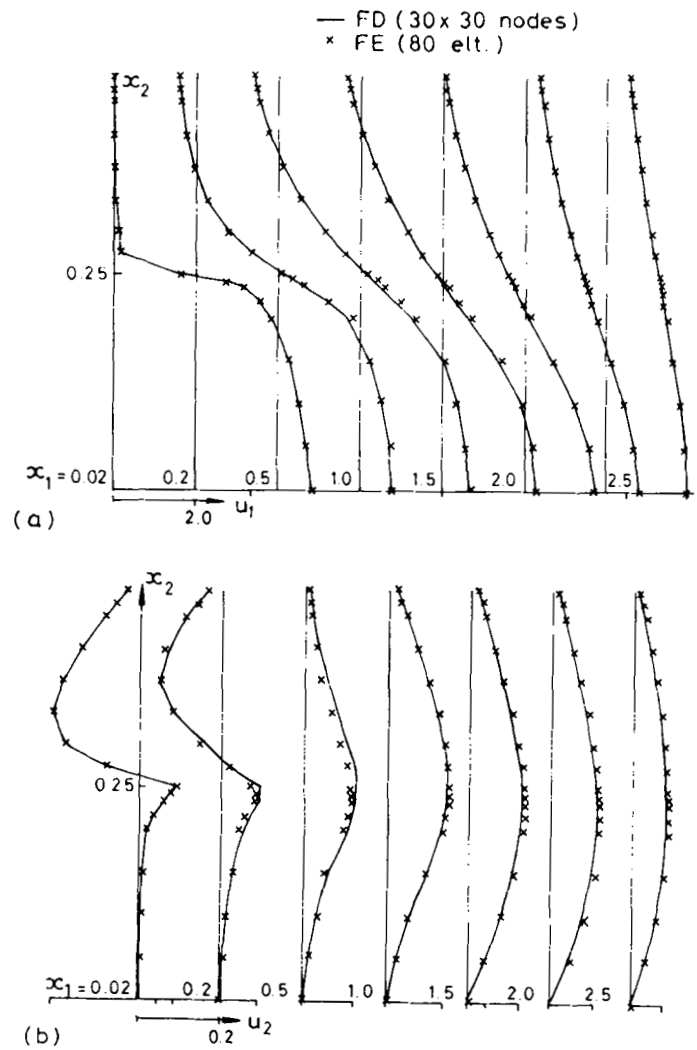

Figure 4. Cross-stream velocity profiles in the sudden pipe-expansion

mesh can resolve the subsequent k and ε variations. The latter is, in fact, achieved by the reduced interpolation of S-model II where, although the total integrated S is unchanged over any element compared with model I, the local peaks are smoothed by the averaging process.

The discrete system generated by S-model II does indeed have a solution for the present flow, shown in Figures 4 and 5. Here, profiles of u_1, u_2, k and ε across the pipe are compared with results from the 30×30 node upwind FD code. It should be noted that interpolated values of the variables from the FD solution have been used as inlet and 'wall' boundary conditions on the FE mesh. Thus, the particular form of wall functions used cannot affect the comparison of results. It can be seen that the velocity profiles from the FE and FD codes are in close agreement. Also, the k and ε fields agree quite closely over most of the expansion, with the important exception of the region just downstream of the re-entrant

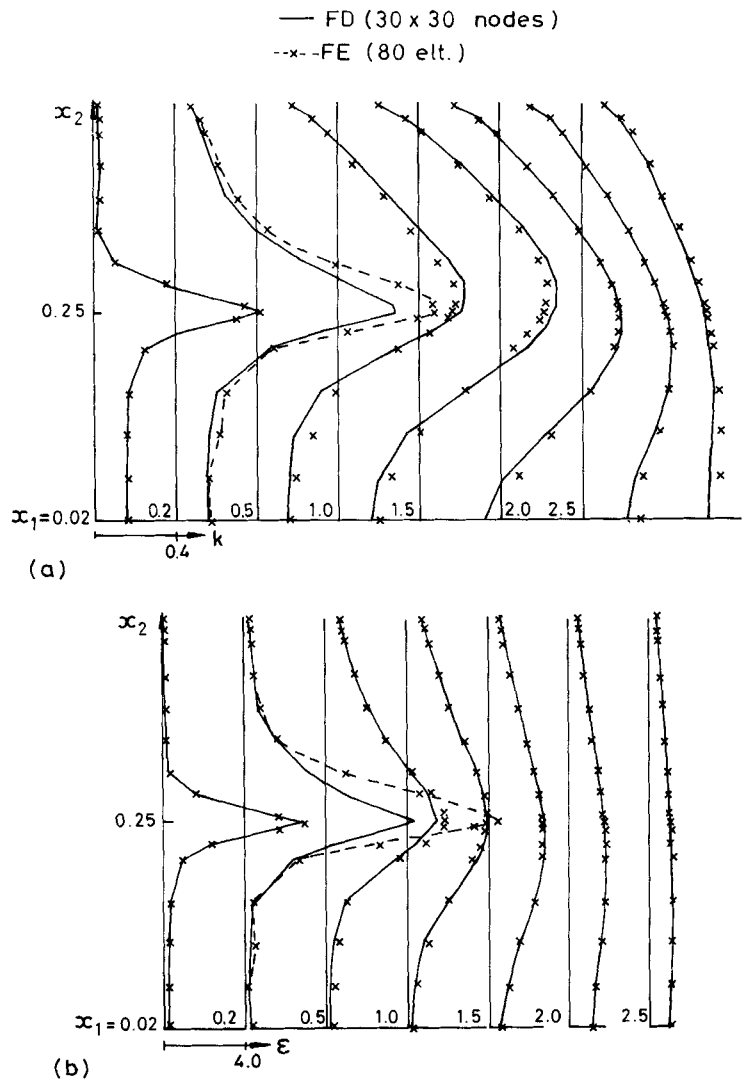

Figure 5. Cross-stream turbulence profiles in the sudden pipe-expansion

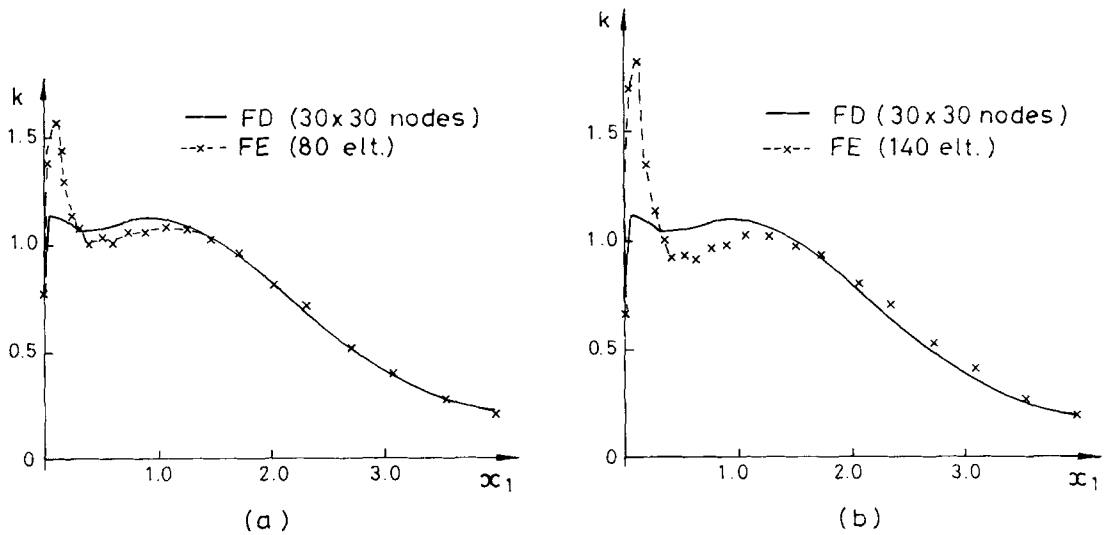

Figure 6. Down-stream profiles of k in the sudden pipe-expansion, $x_2 = 0{\cdot}25$

corner. This is shown more clearly by the downstream profiles from the re-entrant corner in Figures 6(a) and 7(a). The FE solutions show much higher localized peaks than the FD prediction. A grid refinement with fourteen elements across the expansion rather than eight (i.e. a 140 element grid) gives the k and ε downstream profiles shown in Figures 6(b) and 7(b). The peaks downstream of the re-entrant corner are much higher, and it is clear that the 80 element grid is far from grid convergence in this area of the flow. There are changes in the rest of the flow, but these are fairly small compared with those near the corner, and very little adjustment in the velocity predictions results from the refinement.

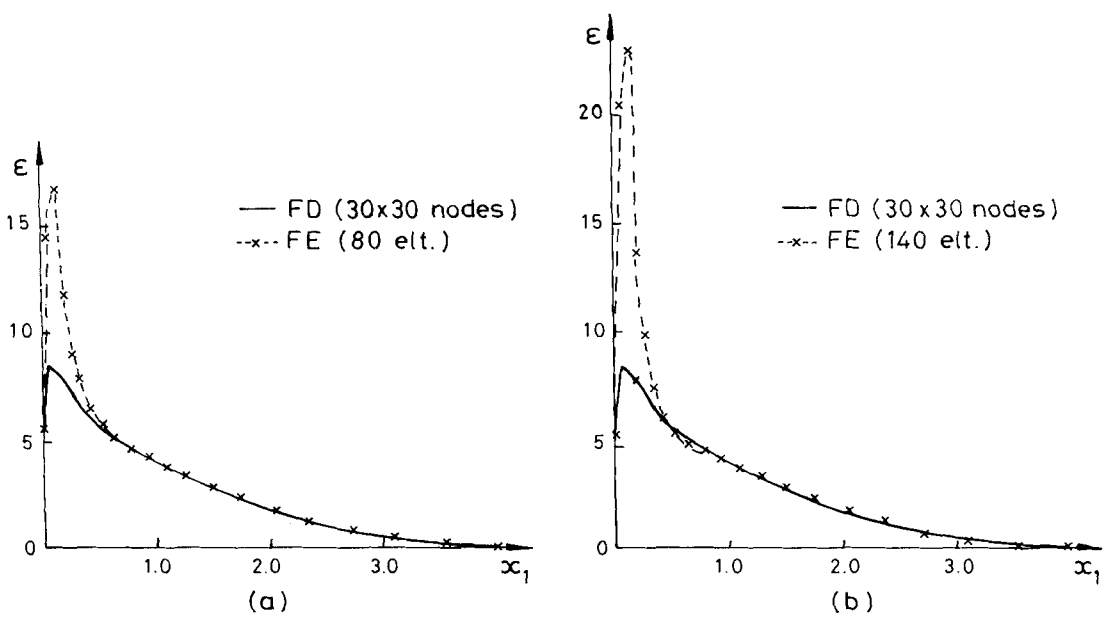

Figure 7. Down-stream profiles of ε in the sudden pipe-expansion, $x_2 = 0{\cdot}25$

Although model II does have discrete solutions on the grids used, convergence of the NR procedure is still very sensitive to the initial guess. For the calculations reported above, the FD results were used to initialize the procedure. Attempts to use the method described in Section 3.2 invariably led to divergence, and this is clearly unacceptable performance.

5. DISCUSSION

5.1. *General considerations*

The performance of the finite-element k–ε code in the calculation of recirculating flow appears most depressing. However there is much to learn from the problems encountered, and this section is consequently the most important part of the paper. Two major difficulties were isolated in the previous section. The first is the occurrence of high localized turbulence levels near the re-entrant corner which can result in the discretized equations having no real solution on a particular mesh. Although reduced interpolation of the S variable does produce a soluble system, it is not clear what level of refinement is necessary to resolve these peaks in k and ε (or indeed whether mesh convergence is attainable). The second difficulty is the extreme numerical instability of the discretized k–ε turbulence model. Problems of this type are often dealt with by using under-relaxed iterative techniques which must often be 'tuned' to a particular flow, but these techniques are unsatisfactory for use in a code designed for practical flow calculations.

Attention is being concentrated on the above problems (dealt with under separate headings below) because they are by no means confined to the present code and discretization method. Cliffe[16] found that solutions to a k–ε finite-element code were unobtainable without the incorporation of artificial diffusivity near a re-entrant corner, and Larock and Schamber[6] and Tong[8] have described serious convergence difficulties. Insight into the causes (and possible cures) of these problems should therefore be of general relevance.

5.2. *Behaviour of the turbulence quantities near the re-entrant corner*

Experimental measurements of normal stresses near a step edge[17–19] indicate that k rises monotonically along the shear layer from the step, reaching a maximum at the value of x_1 which roughly corresponds to reattachment. Such behaviour can be seen in the FE predicted profile for a short distance downstream of the initial peak (see Figure 6(b)). However, there appears to be no experimental evidence for the peak itself, and the numerical results must be judged to be anomalous. Although the magnitudes of the peaks are very different, this anomalous behaviour is predicted by both FE and FD codes, and it is therefore likely that the cause is in the physical modelling.

Boundary conditions are obviously of crucial importance near a re-entrant corner, and it is by no means clear what types of wall functions are appropriate there. However, there is strong evidence that large localized peaks are a feature of the k–ε model in this flow region. It is shown in Appendix I that, in the initial part of the shear layer behind the re-entrant corner, diffusion of the turbulence quantities is small compared with the source terms. If diffusion is neglected, the analytic k–ε equations can be shown to have solutions which grow exponentially along a streamline. Assuming that S and U (the fluid speed) are locally constant along the streamline, Appendix II shows that the exponent is given by $(C_{\varepsilon 2}-C_{\varepsilon 1})(t/U)\sqrt{[C_\mu S(C_{\varepsilon 1}-1)(C_{\varepsilon 2}-1)]}$ where t is distance measured along the streamline. If the recommended constants are adopted, this exponent is positive. Further, as has been pointed

out by Cliffe,[16] near a re-entrant corner S is very large and U will be small. The quantities k and ε can thus be expected to grow rapidly. Appendix I indicates that diffusion of k will be of the same magnitude as production when the level of k in the shear layer is of order 2, and then the conclusions above will no longer be valid. This value is very close to the height ($k_{max} = 1{\cdot}8$) of the anomalous peak in k predicted on the 140 element grid.

As observed above, the peaks in the turbulence quantities are much higher in the FE predictions than those obtained with an upwind-differenced FD code. The details of the source calculation near the boundary could well be responsible for some of the difference, but numerical diffusion, which is an inherent feature of such FD codes, can be expected to damp out large localized peaks. In Galerkin FE codes such features are more obvious (and numerically troublesome) because the artificial damping is not present.

Further investigation of this subject is needed. However, the results presented in Section 4 do demonstrate that the anomalies are highly localized and there is no appreciable effect on the main flow. Thus, the predictions of codes using the k–ε model can still be useful outside the areas of flow showing these anomalous peaks in k and ε.

5.3. *The numerical stability of the discretized k–ε equations*

The solution procedure for the turbulent FE code described in Section 3 uses Newton–Raphson iteration as its basic non-linear solver. Provided that the initial guess is 'close enough', the NR method converges very rapidly, reducing the residual errors quadratically at each iteration. However, rapid convergence does entail large changes in the variables in the initial iterations, and this can take complicated non-linear equations well beyond their range of validity (e.g. k, $\varepsilon < 0$ for the k, ε transport equations). A further hazard is that the discretized equations may have very different types of solutions (if they exist at all) from the original non-linear differential equations. This point is graphically illustrated by the example given in Appendix III. It is shown there that a simple non-linear diffusion equation having a unique analytic solution, when discretized according to the methods described in Section 3, has *multiple* discrete solutions. Among these is a very good approximation to the analytic solution (given a suitable grid), but nearby spurious solutions make it very unlikely that NR iteration, starting from any guess other than the required solution itself, will converge to the correct result. This behaviour is not confined to the particular discretization method employed in the present work. Indeed a centre-differenced replacement (given in Appendix III) of the same differential equation also has multiple solutions. The example described in the Appendix is very simple. In two dimensions and with the much more complicated k–ε system, one would expect similar problems to manifest themselves as a very small radius of convergence for the NR procedure. This was indeed found in the attempts to calculate recirculating flow described in Section 4.

It is clear from these considerations, that, for the NR method to converge reliably from poor guesses, the discretized equation system must be well behaved over a large range of the variables, not just in the vicinity of the required solution. Meyer[20] has examined the solution of a finite-difference replacement of the Dirichlet problem:

$$-\frac{\mathrm{d}}{\mathrm{d}x}\left(\pi(u, x)\frac{\mathrm{d}u}{\mathrm{d}x}\right) - \phi(u, x) = f(x)$$

with $u(0) = u(1) = 0$. Under certain continuity conditions and the requirements

(i) there is a constant $\pi_m > 0$ such that $0 < \pi_m < \pi(u, x)$ uniformly in u and x
(ii) for fixed x, ϕ is monotone decreasing with respect to u

Meyer showed that a solution of the discrete equations exists and is unique. These are the properties one would ideally like for the discrete $k-\varepsilon$ system. So far as the author is aware, there is little equivalent work on finite-element discretizations of non-linear differential equations. However, the basic requirements can be modelled (and their efficacy confirmed) on simple single element discretizations of the type illustrated in Appendix III. If convection is neglected, and the transport equations (6) and (7) are considered separately, it is clear that neither of the basic requirements (i) (uniformly positive diffusivity) nor (ii) (monotone decreasing source term) is satisfied. The diffusivities are negative for $\varepsilon < 0$ and the source terms are increasing with k. A reformulation of the turbulence equations to satisfy the above basic stability properties would clearly have a much better chance of reliable convergence using a fast NR iteration method. Such a reformulation is described in a further paper.[21] which also confirms a vastly improved numerical performance for the resulting turbulent flow code over that reported above.

6. CONCLUSIONS

The performance of the Galerkin FE code described is satisfactory in the simulation of unidirectional flow using the $k-\varepsilon$ turbulence model. However, severe difficulties are encountered with more complex recirculating flow. The underlying causes of these difficulties are as follows:

(i) Extreme local variations of the turbulence quantities are predicted near re-entrant corners by the $k-\varepsilon$ model. In Galerkin FE codes, the resulting overshoots in the numerical approximation can interact with the $k-\varepsilon$ model so that no solution exists on a given mesh. In current finite-difference codes, because of the necessity of upwind differencing, one would expect such variation to be damped out by 'false' diffusion.

(ii) The mathematical form of the $k-\varepsilon$ transport equations leads to discretized systems which are highly unstable with respect to fast converging iterative solution methods (in particular Newton–Raphson).

Successful analysis of these problems has suggested better formulations of the turbulence model equations yielding discretized forms which are numerically stable, and which are therefore suitable for use in practical turbulent flow codes.

ACKNOWLEDGEMENT

This paper is published by permission of the Central Electricity Generating Board.

APPENDIX I. ENERGY BALANCE IN THE MIXING LAYER NEAR A RE-ENTRANT CORNER

The flow just downstream of a re-entrant corner can be considered as a plane mixing layer. Suppose the width of the layer is δ, separating stagnant fluid from a core of velocity u_0, and that inside the layer there is a peak of turbulence energy of magnitude k_m, with $k = k_0$ outside. Using centre-difference approximations, we can now assess the relative magnitudes of the diffsuion and source terms in the transport equations:

$$D_k = \text{Diffusion of } k \approx \frac{\mu_t}{\sigma_k Re}\frac{\partial^2 k}{\partial y^2} \sim \frac{\mu_t}{\sigma_k Re}\frac{8(k_m - k_0)}{\delta^2}$$

$$P_k = \text{Production of } k \approx \frac{\mu_t}{Re}\left(\frac{\partial u}{\partial y}\right)^2 \sim \frac{\mu_t}{Re}\frac{u_0^2}{\delta^2}$$

Thus the ratio $D_k/P_k \sim 8(k_m - k_0)/\sigma_k u_0^2$.

In the present flow, $u_0 \sim 4$ and $(k_m - k_0) \leqslant k_0 = 0{\cdot}16$ at inlet, so the ratio of diffusion of k to production of k is initially $\leqslant 0{\cdot}08$. The ratio is of order unity when $(k_m - k_0) \sim 2$.

APPENDIX II: THE DIFFUSIONLESS k–ε EQUATIONS

An interesting analytic solution of the k–ε equations is available if diffusion is ignored, and S and $|\mathbf{u}| = U$ are assumed constant along a streamline. Then, if t is distance measured along the streamline, the transport equations may be written:

$$U\frac{dk}{dt} = C_\mu \frac{k^2}{\varepsilon} S - \varepsilon \tag{15}$$

$$U\frac{d\varepsilon}{dt} = C_\mu C_{\varepsilon 1} kS - C_{\varepsilon 2}\frac{\varepsilon^2}{k} \tag{16}$$

Introducing $f = \varepsilon/k$, we can write

$$U\frac{df}{dt} = C_\mu(C_{\varepsilon 1} - 1)S - (C_{\varepsilon 2} - 1)f^2 \tag{17}$$

which may be integrated to give

$$f(t) = \sqrt{\left[\frac{SC_\mu(C_{\varepsilon 1}-1)}{(C_{\varepsilon 2}-1)}x\right]} \begin{cases} \tanh(t' - t_0'), & f(t_0) < \sqrt{\left[\dfrac{SC_\mu(C_{\varepsilon 1}-1)}{C_{\varepsilon 2}-1}\right]} \\ \coth(t' - t_0'), & f(t_0) > \sqrt{\left[\dfrac{SC_\mu(C_{\varepsilon 1}-1)}{C_{\varepsilon 2}-1}\right]} \end{cases}$$

where $t' = (t/U)\sqrt{[C_\mu S(C_{\varepsilon 1}-1)(C_{\varepsilon 2}-1)]}$ and t_0 is a constant of integration. This expression may be substituted into equations (15) and (16) to derive expressions for k and ε. In particular, consider the limit of large t', when $f \to \sqrt{\left[\dfrac{SC_\mu(C_{\varepsilon 1}-1)}{(C_{\varepsilon 2}-1)}\right]}$, a constant. Then k and ε behave asymptotically like

$$\exp\left(\frac{(C_{\varepsilon 2} - C_{\varepsilon 1})}{(C_{\varepsilon 1}-1)(C_{\varepsilon 2}-1)}t'\right) \quad \text{where} \quad \frac{C_{\varepsilon 2} - C_{\varepsilon 1}}{(C_{\varepsilon 1}-1)(C_{\varepsilon 2}-1)} > 0$$

with the recommended values of the constants. Thus, as t' becomes large, both k and ε tend exponentially to infinity.

APPENDIX III: DISCRETIZATION OF A NON-LINEAR DIFFUSION EQUATION

Consider the one-dimensional non-linear diffusion equation

$$\frac{d}{dx}\left(\frac{1}{\varepsilon}\frac{d\varepsilon}{dx}\right) = 0, \qquad 0 \leqslant x \leqslant 1 \tag{18}$$

with boundary conditions

$$\varepsilon = \alpha, \qquad x = 0$$
$$\varepsilon = \beta, \qquad x = 1$$

The unique analytic solution is simply:

$$\varepsilon = \varepsilon_0 \exp\left(x \ln \frac{\beta}{\alpha}\right)$$

Consider discretizing equation (18) using the method introduced for the k, ε transport equations, writing

$$\frac{\mathrm{d}}{\mathrm{d}x}\left(\pi \frac{\mathrm{d}\varepsilon}{\mathrm{d}x}\right) = 0 \tag{19}$$

with

$$\pi = \frac{1}{\varepsilon} \tag{20}$$

and interpolating ε and π using quadratic one-dimensional versions $W_i(x)$ of type 2 element basis functions. The Galerkin method is applied to equation (19), and (20) is required to be satisfied at the nodes. This procedure leads to the discrete equations:

$$\frac{\varepsilon_k}{\varepsilon_i} \int \frac{\mathrm{d}W_j}{\mathrm{d}x} \frac{\mathrm{d}W_k}{\mathrm{d}x} W_i \, \mathrm{d}x = 0$$

for the interior nodes and $\varepsilon_j = \alpha$, $\varepsilon_j = \beta$ at the two boundary nodes respectively (where ε_j denotes the value of ε at the jth node). For the trivial case of a single element (i.e. $1 \leq j \leq 3$) there is a single unknown ε_2 given by:

$$\varepsilon_2 = b \pm \sqrt{(b^2 + 2\alpha\beta/3)}$$

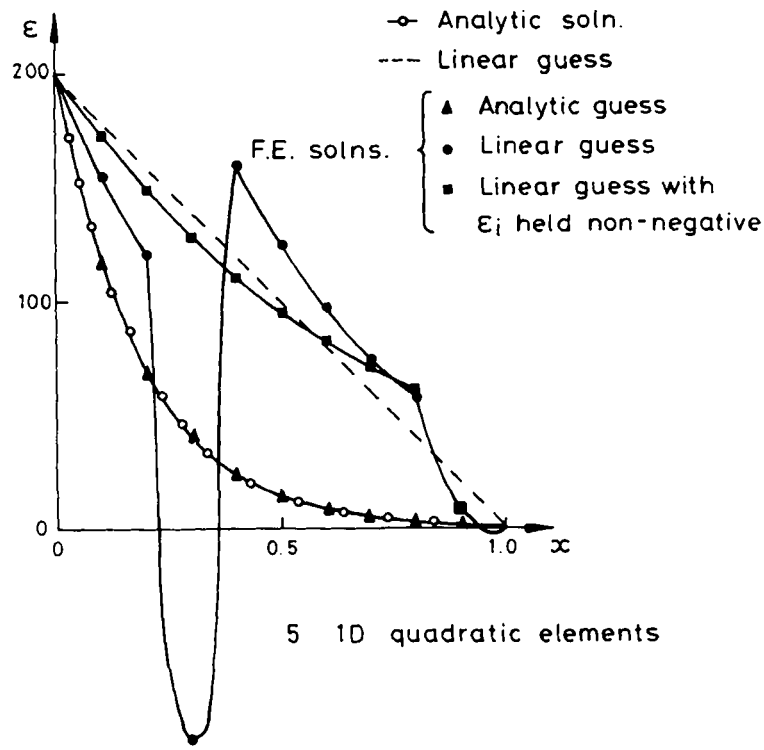

Figure 8. Multiple finite-element solutions obtained by Newton–Raphson

where

$$b = \frac{\alpha^2 + \beta^2 + 6\alpha\beta}{24(\alpha + \beta)}$$

Thus, there are *two* real solutions, one positive and one negative if $\alpha, \beta > 0$. The situation for more than one element is illustrated in Figure 8. Values $\alpha = 200$, $\beta = 1$ are assumed, and the interval [0, 1] is divided into five quadratic elements (i.e. $1 \leq j \leq 11$). If the analytic solution is used as initial guess in the Newton–Raphson procedure, the analytic solution is returned to good accuracy. However, when a linear guess is used, various discrete solutions can be obtained according to the details of the iterative procedure. Thus although the mesh is easily capable of resolving the analytic solution, nearby spurious solutions exist which make it very unlikely that an iterative procedure of the Newton–Raphson type will converge to the required result. Such behaviour is not confined to this particular discretization. For example, the central difference replacement of equation (18)

$$\frac{\varepsilon_{i+1} - \varepsilon_i}{\varepsilon_{i+1} + \varepsilon_i} - \frac{\varepsilon_i - \varepsilon_{i-1}}{\varepsilon_i + \varepsilon_{i-1}} = 0$$

also has multiple solutions.

REFERENCES

1. C. Taylor, K. Morgan and C. A. Brebbia (eds.), *Numerical methods in laminar and turbulent flow, Proc. 1st International Conf.*, Pentech Press, London, 1978.
2. D. H. Norrie (ed.), *Finite elements in flow problems, Proc. 3rd International Conference*, Banff, Canada, 1980.
3. B. E. Launder and D. B. Spalding, *Lectures in mathematical Models of Turbulence*, Academic Press, London, 1972.
4. W. Rodi, *Turbulence models and their application in hydraulics*, IAHR State-of-the-Art Paper, Delft, Netherlands, 1980.
5. A. D. Gosman, W. M. Pun, A. K. Runchal, D. B. Spalding and M. Wolfshtein, *Heat and mass transfer in recirculating flows*, Academic Press, London, 1969.
6. B. E. Larock and D. R. Schamber 'Approaches to the finite element solution of two-dimensional turbulent flows' in C. Taylor and K. Morgan (eds.), *Computational Techniques in Transient and Turbulent Flow*, Pineridge Press, 1981.
7. C. Taylor, C. E. Thomas and K. Morgan, 'Analysis of turbulent flow with separation using the finite element method' in C. Taylor and K. Morgan (eds.), *Computational Techniques in Transient and Turbulent Flow* Pineridge Press, 1981.
8. G. D. Tong, 'Computation of turbulent recirculating flow', *Ph.D. Thesis*, Dept. Civil Engineering, University College of Swansea, U.K., 1982.
9. A. G. Hutton and R. M. Smith, 'On the finite element simulation of incompressible turbulent flow in general two-dimensional geometries', *CEGB Report RD/B/5010N81*, also in C. Taylor and B. A. Schrefler (eds.), *Numerical Methods in Laminar and Turbulent Flow*, Pineridge Press, 1981.
10. W. P. Jones and B. E. Launder 'The prediction of laminarisation with a 2-equation model of turbulence', *Int. J. Heat and Mass Transfer*, **15**, 301 (1972).
11. A. G. Hutton, 'A survey of the theory and application of the finite element method in the analysis of viscous incompressible Newtonian flow', *CEGB Report RD/B/N3049* (1974).
12. O. C. Zienkiewicz, *The Finite Element Method*, 3rd Edn, McGraw Hill, London, 1977.
13. A. G. Hutton and R. M. Smith, 'The prediction of laminar flow over a downstream-facing step by the finite element method', *CEGB Report RD/B/N3660* (1979).
14. J. Barlow, 'Optimal stress locations in finite element models', *Int. J. Num. Meth. Eng.*, **10**, 243–251 (1976).
15. R. T. Szczepura, 'The Reynolds number dependence of the velocity field in the BNL jet-in-pool water experiments', *CEGB Report RD/B/4999N81* (1981).
16. A. Cliffe, Private Communication (1979).
17. J. J. Kim, 'Investigation of separation and reattachment of a turbulent shear layer: flow over a backward-facing step, *Ph.D. thesis*, Stanford University, 1978.
18. C. Chandrsuda, 'A reattaching turbulent shear layer in incompressible flow', *Ph.D. thesis*, Dept. of Aeronautics, Imperial College, London, 1975.

19. R. T. Szczepura, Private communication (1982).
20. G. H. Meyer, 'The numerical solution of quasilinear elliptic equations' in G. D. Byrne and C. A. Hall (eds.), *Numerical Solution of Systems of Nonlinear Algebraic Equations*, Academic Press, New York, 1973.
21. R. M. Smith, 'A practical method of two-equation turbulence modelling using finite elements', *Int. j. numer. methods fluids*, **4**, 321–336 (1984).